

Training Multi-Layer Binary Neural Networks With Local Binary Error Signals

Luca Colombo^{a,*}, Fabrizio Pittorino^a, Manuel Roveri^a

^a*Department of Electronics, Information and Bioengineering, Politecnico di Milano, Via Ponzio
34/5, Milano, 20133, Italy*

Abstract

Binary Neural Networks (BNNs) hold the potential for significantly reducing computational complexity and memory demand in machine and deep learning. However, most successful training algorithms for BNNs rely on quantization-aware floating-point Stochastic Gradient Descent (SGD), with full-precision hidden weights used during training. The binarized weights are only used at inference time, hindering the full exploitation of binary operations during the training process. In contrast to the existing literature, we introduce, for the first time, a multi-layer training algorithm for BNNs that does not require the computation of back-propagated full-precision gradients. Specifically, the proposed algorithm is based on local binary error signals and binary weight updates, employing integer-valued hidden weights that serve as a synaptic metaplasticity mechanism, thereby establishing it as a neurobiologically plausible algorithm. The binary-native and gradient-free algorithm proposed in this paper is capable of training binary multi-layer perceptrons (BMLPs) with binary inputs, weights, and activations, by using exclusively XNOR, Popcount, and increment/decrement operations, hence effectively paving the way for a new class of operation-optimized training algorithms. Experimental results on BMLPs fully trained in a binary-native and gradient-free manner on multi-class image classification benchmarks demonstrate an accuracy improvement of up to +13.36% compared to the fully binary state-of-the-art solution, showing minimal accuracy degradation compared to the same architecture trained with full-precision SGD and floating-point weights, activations, and inputs. The proposed algorithm is made available to the scientific community as a public repository.

Keywords: Binary Neural Networks, Gradient-free learning, Binary-native learning, Neurobiologically plausible training

1. Introduction

In recent years, Machine Learning (ML) and Deep Learning (DL) models are becoming more and more accurate in solving increasingly challenging tasks, as well as more and more

*Corresponding author.

Email addresses: luca2.colombo@polimi.it (Luca Colombo), fabrizio.pittorino@polimi.it (Fabrizio Pittorino), manuel.roveri@polimi.it (Manuel Roveri)

complex in terms of number of parameters, which translates into higher computational demand, memory usage and energy consumption (Thompson Neil et al., 2020; Simonyan and Zisserman, 2014). A promising approach that tries to overcome this drawback is represented by quantization, which aims at reducing the precision of model weights and/or activations from floating-point values to low-bit integers, resulting in model compression and faster execution (Hubara et al., 2018; Jacob et al., 2018).

Binary Neural Networks (BNNs) are the simplest and most extreme version of low-bit quantized models. Specifically, they represent weights and activations exclusively with binary values (typically -1 and +1), significantly reducing memory usage. Moreover, BNNs exploit the efficiency of bitwise operations, such as XNOR and Popcount, to perform multiplications and additions, drastically reducing the computational complexity and energy demand compared to their full-precision counterparts (Qin et al., 2020).

The literature in this field mainly introduces works in which BNNs are employed only during the inference phase, exploiting quantization aware-training techniques for the learning phase (Yuan and Aghaian, 2023). In this perspective, full-precision floating-point Stochastic Gradient Descent (SGD) is used to optimize the floating-point model parameters during the backward pass, while the weights are binarized only during the forward pass (Courbariaux et al., 2015; Rastegari et al., 2016). Only one work present in the literature introduces an alternative binary-native method to learn a single fully-connected layer, although it is limited to BNNs composed of only a single hidden layer (Baldassi et al., 2015).

In this perspective, the aim of this paper is to address the following research question: *can we train multi-layer BNNs in a binary-native and gradient-free manner?* To the best of our knowledge, we propose, for the first time in the literature, a novel binary-native and gradient-free learning algorithm capable of training Binary Multi-layer Perceptrons (BMLPs). In particular, by enhancing the Clipped Perceptron with Reinforcement (CP+R) rule (Baldassi, 2009) and Local Error Signals (LES) (Nøkland and Eidnes, 2019), the proposed algorithm is able to train multiple layers of a BMLP using random binary local classifiers while employing only XNOR, Popcount, and increment/decrement operations. Specifically, inputs, weights, activations, and weight updates are all represented with binary values. To avoid the catastrophic forgetting issue (Kirkpatrick et al., 2017), integer-valued hidden weights are employed, acting as a synaptic metaplasticity mechanism. This mechanism, along with local learning signals, enhances the algorithm’s neurobiological plausibility (Braunstein and Zecchina, 2006; Nøkland, 2016).

In summary, the proposed solution introduces the following innovations:

1. A novel BMLP model with random binary and fixed local classifiers supporting the binary-native inference and training.
2. A binary-native and gradient-free learning algorithm specifically designed to train the proposed BMLP.

Consequently, the proposed solution: *(i)* enables the training of BMLP by discarding the traditional full-precision floating-point SGD algorithm, *(ii)* allows deep BMLP learning by training multiple layers independently, paving the way for the binary training of state-of-the-art models, and *(iii)* allows for the exclusive exploitation of efficient binary operations,

Table 1: Comparison with existing solutions. †: exploit full-precision in/out layers or scaling-factors

Algorithm	Binary forward	Binary backward	Multi-layer architectures
(Courbariaux et al., 2015)	Yes [†]	No	Yes
(Rastegari et al., 2016)	Yes [†]	No	Yes
(Lin et al., 2017)	Yes [†]	No	Yes
(Bulat and Tzimiropoulos, 2019)	Yes [†]	No	Yes
(Liu et al., 2020)	Yes [†]	No	Yes
(Tu et al., 2022)	Yes [†]	No	Yes
(Lin et al., 2022)	Yes [†]	No	Yes
(Vargas et al., 2024)	Yes [†]	No	Yes
(Baldassi et al., 2015)	Yes	Yes	No
Proposed solution	Yes	Yes	Yes

such as XNOR, Popcount, and increment/decrement operations, *even during the learning phase*, hence drastically reducing computational complexity and execution time.

Experimental results on BMLPs trained with the proposed solution on multi-class image classification benchmarks demonstrate both an accuracy improvement of up to +13.36% compared to the state-of-the-art single-hidden layer BNN (Baldassi et al., 2015), and minimal accuracy degradation compared to the same architecture trained with full-precision SGD and floating-point weights, activations, and inputs.

The paper is organized as follows. In Section 2, an overview on the related literature is given. Section 3 presents the proposed solution, while experimental results are shown in Section 4. Conclusions are finally drawn in Section 5.

2. Related literature

This section describes the related literature in the field of BNNs, with existing works grouped into two main categories: BNNs enabling binary forward pass but employing full-precision SGD during the backward pass, and BNNs enabling both binary forward and binary backward passes, relying on neurobiologically plausible rules. Solutions belonging to these two categories are summarized and analyzed in Table 1.

Most of the literature focuses on the first category. More specifically, the concept of binary neural networks was pioneered by (Courbariaux et al., 2015), who proposed the binarization of weights and activations using the *sign* function and replacing most arithmetic operations in deep neural networks with bit-wise operations. To minimize the quantization error, XNOR-Net (Rastegari et al., 2016) introduced a channel-wise floating-point scaling factor for reconstructing the binarized weights, which has become a crucial component of subsequent BNNs. ABC-Net (Lin et al., 2017) approximated full-precision weights using a linear combination of multiple binary weight bases and employed multiple binary activations to mitigate information loss. Inspired by the architectures of ResNet (He et al., 2016) and

DenseNet (Huang et al., 2017), Bi-Real Net (Liu et al., 2020) incorporated shortcuts to bridge the performance gap between 1-bit and real-value CNN models. AdaBin (Tu et al., 2022) adaptively obtains the optimal binary sets $\{\pm\alpha\}$ of weights and activations for each layer, with $\alpha \in \mathbb{R}$, instead of a fixed set $\{\pm 1\}$. Specifically, as summarized in Table 1, these solutions, along with others (Bulat and Tzimiropoulos, 2019; Li et al., 2022; Lin et al., 2022; Vargas et al., 2024), employ binary weights and activations only during the forward pass, while full-precision SGD is used to optimize floating-point model parameters during the backward pass. Moreover, most of them exploit floating-point scaling factors or floating-point weights in the input/output layer to reduce accuracy degradation. Differently, our proposed solution provides a gradient-free algorithm capable of training multi-layer BNNs by performing a fully binarized forward and backward passes.

The second category comprises works which enable both binary forward and binary backward passes. Interestingly, only one work (Baldassi et al., 2015) is present in this category. In particular, it supports the training of a single layer in a single-hidden layer BNN by adopting a custom and fixed neural network architecture along with a training algorithm based on the CP+R rule. This architecture is organised as: a first fully-connected layer (i.e., the layer being trained), a custom sparse grouping layer which groups together perceptrons from the previous layer, and a final fully-connected random classifier. The training algorithm exploits the CP+R rule, a gradient-free procedure that simplifies the training of single binary perceptrons to the extreme, adhering to a stream of literature that aims toward neurobiological plausibility (Rosen-Zvi, 2000; Baldassi et al., 2007; Baldassi, 2009). Despite being of interest, (Baldassi et al., 2015) provides a solution that cannot be directly extended to multi-layer BNNs, given the rigidity of the neural network architecture and the training algorithm tailored to that specific architecture. Conversely, as summarized in Table 1, our proposed solution overcomes these limitations by relaxing the constraints on the network architecture, which can scale up to an unlimited number of hidden layers, and by providing a generalized binary-native learning algorithm able to train multi-layer BNNs.

3. Proposed solution

This section presents our proposed binary-native and gradient-free algorithm for training BMLPs. Specifically, the proposed algorithm operates at three different levels:

1. The *network* level, where the forward pass takes place and the local loss functions are computed to identify layers committing an error.
2. The *layer* level, operating independently for each layer identified at the previous step, where the perceptrons to be updated are selected.
3. The *perceptron* level, operating independently for each layer and for each previously identified perceptron, where the weights are updated.

Section 3.1 details the architecture of the BMLP under consideration. Section 3.2, Section 3.3, and Section 3.4 explain the proposed algorithm at the network, layer and perceptron level, respectively. Lastly, Section 3.5 provides an overview of the computational costs and memory footprint of the proposed solution.

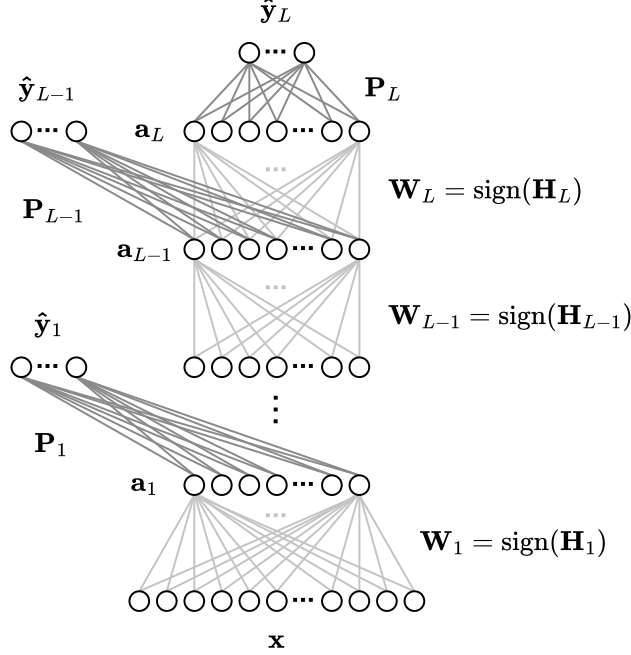


Figure 1: The proposed BMLP architecture. \mathbf{H}_l , \mathbf{W}_l , \mathbf{P}_l , \mathbf{a}_l , and $\hat{\mathbf{y}}_l$ are the hidden integer metaplastic weights, the binary weights, the random classifier binary weights, the activations, and the local block output of layer l , with $l = 1, \dots, L$, respectively. \mathbf{x} is the binary input.

3.1. Architecture and visible and hidden weights

The proposed binary-native and gradient-free learning algorithm is designed for the training of BMLPs on multi-class classification problems defined on a dataset $\mathbf{X} = \{\mathbf{x}^\mu, y^\mu\}_{\mu=1}^P$, where $\mathbf{x}^\mu \in \mathbb{R}^{K_0}$ are the input patterns of dimension K_0 , $y^\mu \in \{1, \dots, c\}$ their corresponding labels (where c is the number of classes), and P is the size of the training set.

The proposed BMLP architecture, inspired by LES (Nøkland and Eidnes, 2019), is shown in Figure 1. Let L be the total number of fully-connected layers within the considered BMLP, and let K_l be the dimension of layer $l \in \{1, \dots, L\}$. It should be noted that the input dimension of the BMLP is K_0 , while the output dimension is c . Inspired by (Baldassi, 2009), each layer l is represented by two matrices: the hidden metaplastic integer weights \mathbf{H}_l of size $K_{l-1} \times K_l$, which are updated during the backward pass, and the binary weights \mathbf{W}_l , where $\mathbf{W}_l = \text{sign}(\mathbf{H}_l)$, that are used in the forward pass. The hidden metaplastic variables $h \in \mathbf{H}_l$ can be interpreted as the *confidence* of each binary weight in assuming its current value, as the larger the absolute value of h , the more difficult for the variable w to change its sign.

Each fully-connected layer l is also associated with a fixed random classifier \mathbf{P}_l of size $K_l \times c$, which is a fully-connected layer with weights ρ uniformly drawn from $\{\pm 1\}$. The objective of these random classifiers is to reduce the dimension of the activations \mathbf{a}_l of the l -th layer to match the output dimension c and produce the local output $\hat{\mathbf{y}}_l$, which is used during the backward pass by the local loss function \mathcal{L} , along with the true label y , to compute the local error ℓ_l . This local error is then used by the training algorithm to

compute the weight updates of layer l . In the last layer (i.e., $l = L$), the random classifier \mathbf{P}_L serves as the final output layer, where the network output $\hat{\mathbf{y}}_L$ is produced and the final accuracy is evaluated. Once the training phase is completed, the intermediate random classifiers \mathbf{P}_l , with $l \in \{1, \dots, L - 1\}$, can either be discarded or employed for early exit strategies (Teerapittayanon et al., 2016; Scardapane et al., 2020; Casale and Roveri, 2023). We emphasize that, if all layers L share the same dimension K_l , a unique random classifier \mathbf{P} can be considered for the training phase.

It is worth noting that this architecture enables the independent training of each layer and allows the parallelization of the training procedure. Moreover, it allows the binary training of arbitrarily deep BMLPs, as explained in the following sections.

3.2. Network-level: forward pass, robustness and local loss

The first step of the proposed binary-native and gradient-free learning algorithm operates at the network level. Specifically, as detailed in Algorithm 1, it works as follows. First, for each layer l , the hidden metaplastic weights \mathbf{H}_l and the random classifier weights \mathbf{P}_l are initialized with random weights uniformly sampled from $\{\pm 1\}$ (see line 2). Second, for each mini-batch $(\mathbf{x}, \mathbf{y}) \subseteq \mathbf{X}$, with $|\mathbf{x}| = |\mathbf{y}| = bs$, where bs is the mini-batch size, the input patterns \mathbf{x} are binarized into \mathbf{a}_0 using the median value as a threshold¹, resulting in $\mathbf{a}_{0,i}^\mu \in \{\pm 1\}$, $\mu \in \{1, \dots, bs\}$, $i \in \{1, \dots, K_0\}$ (see line 5). Third, the set of pattern indexes to update \mathcal{M}_l is defined and initialized as the empty set \emptyset (see line 7). At this point, the forward pass begins. For each layer $l \in \{1, \dots, L\}$, the algorithm computes the pre-activations $\mathbf{z}_l = \mathbf{a}_{l-1} \text{sign}(\mathbf{H}_l)$, the activations $\mathbf{a}_l = \text{sign}(\mathbf{z}_l)$, and the local output $\hat{\mathbf{y}}_l = \mathbf{a}_l \mathbf{P}_l$ (see lines 8-10). It then evaluates, for each pattern index $\mu \in \{1, \dots, bs\}$, whether the l -th layer correctly classifies the binary input pattern \mathbf{a}_0^μ by computing the *01-Loss* $\ell_l^\mu = \mathcal{L}_{0/1}(\hat{\mathbf{y}}_l^\mu, y^\mu)$ defined as follows:

$$\mathcal{L}_{0/1}(\hat{\mathbf{y}}^\mu, y^\mu) = \begin{cases} 0 & \text{if } \arg \max(\hat{\mathbf{y}}^\mu) = y^\mu \\ 1 & \text{if } \arg \max(\hat{\mathbf{y}}^\mu) \neq y^\mu \end{cases}, \quad (1)$$

where $\hat{\mathbf{y}}^\mu$ is the local output of layer l and y^μ is the true label, namely, the desired output. In addition to the computation of the *01-Loss* ℓ_l^μ , a stronger correctness constraint can be enforced by introducing a robustness parameter r . This user-specified hyperparameter is compared to the difference between the first and the second highest local output values $\tau_l^\mu = \hat{\mathbf{y}}_{l(c)}^\mu - \hat{\mathbf{y}}_{l(c-1)}^\mu$, which can be interpreted as the confidence of the l -th layer in classifying the considered pattern \mathbf{a}_0^μ . If the μ -th pattern is correctly classified, i.e., $\ell_l^\mu = 0$, with a confidence over the robustness threshold, i.e., $\tau_l^\mu \geq rK_l$ (notice that r is scaled by the layer size K_l) by the l -th layer, no weight update is carried out. Otherwise, the index μ is added to the set of pattern indexes to update \mathcal{M}_l of layer l (see line 15). Once the mini-batch has

¹Although alternative binarization methods can be considered, it is also feasible to adapt the BMLP to handle directly integer and floating-point inputs. This can be accomplished by adding a fixed and random expansion layer with weights in $\{\pm 1\}$ as the input layer of the BMLP.

Algorithm 1: Proposed network-level BMLP training algorithm

Data: \mathbf{X} : training data
Variables: L : number of layers, K_l : number of perceptrons in layer l , \mathbf{H}_l : hidden metaplastic weights in layer l , \mathbf{P}_l : random classifier weights associated to layer l , E^e : fraction of training errors at epoch e
Hyperparameters: e : number of epochs, bs : mini-batch size, r : robustness, γ : group size, p_r : reinforcement probability

```
1 def NetworkUpdate( $\mathbf{X}, L, e, bs, r, \gamma, p_r$ ):
2   Initialize  $\{\mathbf{H}_l, \mathbf{P}_l\}$  foreach layer  $l = 1, \dots, L$ 
3   foreach epoch  $e$  do
4     foreach  $(\mathbf{x}, \mathbf{y}) \subseteq \mathbf{X}, |\mathbf{x}| = |\mathbf{y}| = bs$  do
5       Binarize input data  $\mathbf{a}_0 = \text{MedianBinarization}(\mathbf{x})$ 
6       foreach  $l = 1, \dots, L$  do
7         Initialize set of pattern indexes to update  $\mathcal{M}_l \leftarrow \emptyset$ 
8         Compute pre-activations  $\mathbf{z}_l = \mathbf{a}_{l-1} \text{sign}(\mathbf{H}_l)$ 
9         Compute activations  $\mathbf{a}_l = \text{sign}(\mathbf{z}_l)$ 
10        Compute local output  $\hat{\mathbf{y}}_l = \mathbf{a}_l \mathbf{P}_l$ 
11        foreach  $\mu = 1, \dots, bs$  do
12          Compute local 01-Loss  $\ell_l^\mu = \mathcal{L}_{0/1}(\hat{\mathbf{y}}_l^\mu, y^\mu)$ 
13          Compute  $\tau_l^\mu = \hat{\mathbf{y}}_{l(c)}^\mu - \hat{\mathbf{y}}_{l(c-1)}^\mu$ 
14          if  $\ell_l^\mu = 1$  or  $\tau_l^\mu < rK_l$  then
15            | Add  $\mu$  to set of pattern indexes to update  $\mathcal{M}_l \leftarrow \mathcal{M}_l \cup \{\mu\}$ 
16          end
17        end
18        LayerUpdate( $\mathbf{a}_{l-1}, \mathbf{y}, \mathbf{z}_l, \mathcal{M}_l, l, \gamma, p_r$ )
19      end
20    end
21    Rescale probability  $p_r = p_r \sqrt{E^e}$ 
22  end
```

been entirely processed, the algorithm proceeds at the layer-level by updating each layer l simultaneously using its set \mathcal{M}_l , as described in the next section.

3.3. Layer-level

If the set of pattern indexes to update $\mathcal{M}_l \neq \emptyset$ in a given layer l , i.e., $\ell_l^\mu = 1$ or $\tau_l^\mu < rK_l$ for at least one binary input pattern \mathbf{a}_0^μ , with $\mu \in \{1, \dots, bs\}$, as described in the previous section, the layer-level algorithm is executed. In particular, as detailed in Algorithm 2 and illustrated in Figure 2, it works as follows. First, the K_l perceptrons are divided into G sub-groups of size γ , where γ is a user-specified hyperparameter and $G = \frac{K_l}{\gamma}$ (see line 2). The role of γ will be analyzed extensively in Section 4.2. Second, the set of perceptron indexes to update \mathcal{U}_l is defined and initialized as the empty set \emptyset (see line 3).

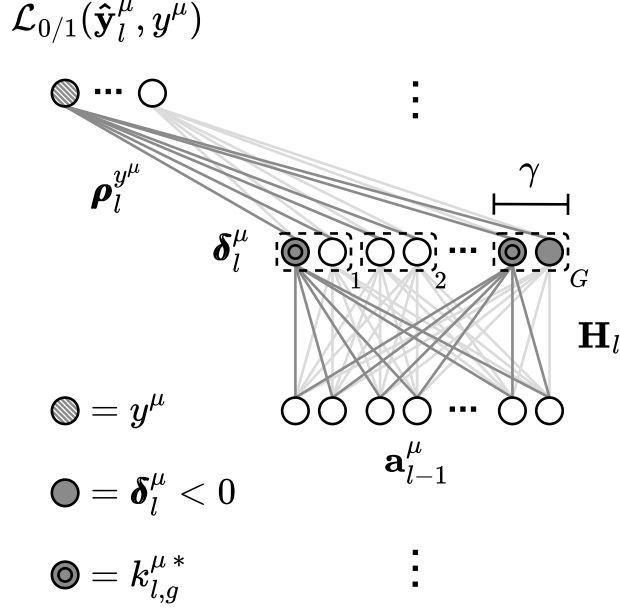


Figure 2: Proposed binary-native and gradient-free learning algorithm operating at the layer level. \mathbf{H}_l are the hidden integer metaplastic weights, \mathbf{a}_{l-1} are the activations of the previous layer, G is the number of sub-groups, γ is the group size, y^μ is the true label of μ -th pattern, $\rho_l^{y^\mu}$ are the random classifier weights associated to the true label, δ_l^μ are the local stabilities, and $k_{l,g}^{\mu*}$ are the *easiest* perceptrons to update within each sub-group g .

Third, each perceptron $k \in \{1, \dots, K_l\}$ is examined to identify those contributing to the error of its associated random classifier \mathbf{P}_l . Specifically, the perceptrons contributing to the error are characterized by a negative product δ_l^μ of their pre-activations $\mathbf{z}_{l,k}^\mu$ and the random classifier weights associated with the true label $\rho_l^{y^\mu}$. In other words, for each pattern $\mu \in \mathcal{M}_l$, the perceptrons for which the local stabilities $\delta_l^\mu = \mathbf{z}_{l,k}^\mu \rho_l^{y^\mu} < 0$ are considered (see line 5). Lastly, within each sub-group $g \in \{1, \dots, G\}$, only the *easiest* perceptron to fix is selected (i.e., the one with the negative stability closest to 0), whose index is given by $k_{l,g}^{\mu*} \in \arg \max_{k \in g} (\delta_l^\mu : \delta_l^\mu < 0)$ (see line 7). The selected perceptron indexes, which amount to at most G (i.e., when there is at least one perceptron contributing to the error per group), along with their corresponding pattern index μ , are added to the set \mathcal{U}_l (see line 8). Once every $\mu \in \mathcal{M}_l$ has been processed, the set \mathcal{U}_l contains at most $G \times bs$ tuples, each of which contains the pattern index μ and the perceptron index $k_{l,g}^{\mu*}$ (e.g., $\mathcal{U}_l = \{(\mu_1, k_{l,1}^{\mu_1*}), \dots, (\mu_1, k_{l,G}^{\mu_1*}), \dots, (\mu_{bs}, k_{l,1}^{\mu_{bs}*}), \dots, (\mu_{bs}, k_{l,G}^{\mu_{bs}*})\}$). These tuples are then used by the perceptron-level algorithm to perform the updates, as described in the next section.

3.4. Perceptron level

Once the perceptrons to update \mathcal{U}_l have been selected for each layer l , as described in the previous section, the proposed algorithm proceeds at the perceptron level. Specifically, as detailed in Algorithm 3, it relies on the two steps of the CP+R rule (Baldassi, 2009). First, for each tuple $(\mu, k_{l,g}^{\mu*}) \in \mathcal{U}_l$, it updates the hidden metaplastic weights $\mathbf{h}_l^{k_{l,g}^{\mu*}}$ (i.e., those

Algorithm 2: Proposed layer-level BMLP training algorithm

Variables: $\rho_l^{y^\mu}$: random classifier weights in layer l associated to the true label y^μ of the μ -th pattern

```
1 def LayerUpdate( $\mathbf{a}_{l-1}, \mathbf{y}, \mathbf{z}_l, \mathcal{M}_l, l, \gamma, p_r$ ):
2    $\mathcal{G} \leftarrow$  (split  $K_l$  into  $G$  groups of size  $\gamma$ )
3   Initialize set of perceptron indexes to update  $\mathcal{U}_l \leftarrow \emptyset$ 
4   foreach  $\mu$  in  $\mathcal{M}_l$  do
5     Compute perceptron local stabilities  $\delta_l^\mu = \mathbf{z}_l^\mu \rho_l^{y^\mu}$ 
6     foreach  $g$  in  $\mathcal{G}$  do
7       Find easiest perceptron to fix  $k_{l,g}^{\mu*} = \arg \max_{k \in g} (\delta_l^\mu : \delta_l^\mu < 0)$ 
8       Add  $(\mu, k_{l,g}^{\mu*})$  to set of perceptron indexes to update  $\mathcal{U}_l \leftarrow \mathcal{U}_l \cup \{(\mu, k_{l,g}^{\mu*})\}$ 
9     end
10  end
11  PerceptronUpdate( $\mathbf{a}_{l-1}, \mathbf{y}, \mathcal{U}_l, l, p_r$ )
```

Algorithm 3: Perceptron-level BMLP training algorithm (Baldassi, 2009)

Variables: \mathbf{h}_l^k : hidden metaplastic weights in layer l associated to perceptron k

```
1 def PerceptronUpdate( $\mathbf{a}_{l-1}, \mathbf{y}, \mathcal{U}_l, l, p_r$ ):
2   // Clipped Perceptron
3   foreach  $(\mu, k_{l,g}^{\mu*})$  in  $\mathcal{U}_l$  do
4     Update  $\mathbf{h}_l^{k_{l,g}^{\mu*}} \leftarrow \mathbf{h}_l^{k_{l,g}^{\mu*}} + 2 \mathbf{a}_{l-1}^\mu \rho_l^{y^\mu, k_{l,g}^{\mu*}}$ 
5   end
6   // Reinforcement
7   foreach  $k = 1, \dots, K_l$  do
8     foreach  $h$  in  $\mathbf{h}_l^k$  do
9       Extract  $p \leftarrow \text{Uniform}(0, 1)$ 
10      if  $p < p_r \sqrt{\frac{2}{\pi K_l}}$  then
11         $h \leftarrow h + 2 \text{sign}(h)$ 
12      end
13    end
14  end
```

associated with the previously selected perceptron $k_{l,g}^{\mu*}$) by using the Clipped Perceptron (CP) rule, i.e., $\mathbf{h}_l^{k_{l,g}^{\mu*}} \leftarrow \mathbf{h}_l^{k_{l,g}^{\mu*}} + 2 \mathbf{a}_{l-1}^\mu \rho_l^{y^\mu, k_{l,g}^{\mu*}}$ (see lines 2-4). Second, it computes the Reinforcement (R) rule of each metaplastic hidden weight $h \in \mathbf{H}_l$ according to the reinforcement probability p_r , i.e., $h \leftarrow h + 2 \text{sign}(h)$ (see lines 5-12). At the end of each epoch e , the reinforcement probability p_r is rescaled by a factor $\sqrt{E^e}$, where E^e is the fraction of training errors made by the BMLP during the current epoch e (Baldassi, 2024).

Table 2: Computational costs of the proposed solution in terms of number of operations for each layer $l = \{1, \dots, L\}$ and for each input pattern \mathbf{a}_0^μ . K_l and K_{l-1} are the sizes of layer $l-1$ and layer l , respectively. c is the number of classes, and γ is the group size.

Operation	Number of operations	
	Forward	Backward
XNOR	$K_l(K_{l-1} + c)$	$K_l \left(1 + \frac{K_{l-1}}{\gamma}\right)$
Popcount	$K_l + c$	-
Increment/decrement	-	$2 \frac{K_l K_{l-1}}{\gamma}$

Table 3: Memory footprint of the proposed solution in terms of number of bits needed for representing each value. \mathbf{a}_l are the activations, and \mathbf{h}_l and \mathbf{w}_l are the integer-valued integer metaplastic weights and the binary weights, respectively. The hidden weights \mathbf{h}_l are used only during the backward pass, while the binary weights \mathbf{w}_l are used only during the forward pass.

Variable	Number of bits	
	Forward	Backward
\mathbf{a}_l	1	1
\mathbf{h}_l	-	8
\mathbf{w}_l	1	-

3.5. Computational costs and memory footprint

The proposed binary-native and gradient-free learning algorithm offers two key advantages w.r.t. full-precision SGD. Firstly, from a computational perspective, it enables the exploitation of efficient binary operations even during the training phase, thereby drastically reducing computational complexity and execution time. Specifically, it is capable of training a BMLP relying solely on XNOR, Popcount, and increment/decrement operations. Table 2 illustrates the number of operations required to process a single input pattern \mathbf{a}_0^μ for each layer l , both in the forward and the backward passes. Second, from a memory perspective, it reduces the memory footprint of both the training procedure and the final model. Specifically, as summarized in Table 3, the activations \mathbf{a}_l and the binary weights \mathbf{w}_l require only 1-bit values, while the integer-valued hidden metaplastic weights \mathbf{h}_l require 8-bit values. It is worth noting that, similarly to all the other BNN-related works present in the literature (Rastegari et al., 2016; Baldassi et al., 2015), the pre-activations \mathbf{z}_l require $\lceil \log_2(2K_{l-1}) \rceil$ bits to be represented. Nonetheless, the values of \mathbf{z}_l can be bounded by taking a number of bits equals to $\min_{l \in \{1, \dots, L\}} (8, \lceil \log_2(2K_{l-1}) \rceil)$, without compromising the final accuracy.

We emphasize that the proposed algorithm can be implemented by using bit-shift operations instead of increment/decrement operations, albeit at the cost of increasing the number of bits of the integer-valued hidden metaplastic weights \mathbf{h}_l to provide a sufficient number of possible levels.

4. Experimental results

In this section, we evaluate the effectiveness of the proposed multi-layer binary-native and gradient-free training algorithm. The goal of this experimental campaign is to demonstrate that the proposed solution not only surpasses the performance of the state-of-the-art algorithm (Baldassi et al., 2015), but also achieves performance close to that of traditional floating-point MLPs trained with full-precision SGD. Specifically, Section 4.1 details the datasets employed in the experiments. In Section 4.2, the proposed algorithm is compared with both (Baldassi et al., 2015) and full-precision SGD. Section 4.2 provides an analysis of the role of the group size γ , showing its influence in the training procedure. In Section 4.4, an ablation study considering enhanced versions of the SOTA algorithm is carried out. Lastly, in Section 4.5, the proposed algorithm is compared with full-precision SGD when dealing with deep architectures.

The Python code of the experiments performed in this paper is made available to the scientific community as a public repository ².

4.1. Datasets

4.1.1. MNIST

The first dataset considered is the MNIST (Modified National Institute of Standards and Technology) database (LeCun, 1998), a widely used dataset consisting of handwritten digit images. The elements are grey-scale images with a size of 28×28 pixels. The dataset comprises 60000 training samples and 10000 testing samples from 10 different classes, each representing a digit from 0 to 9.

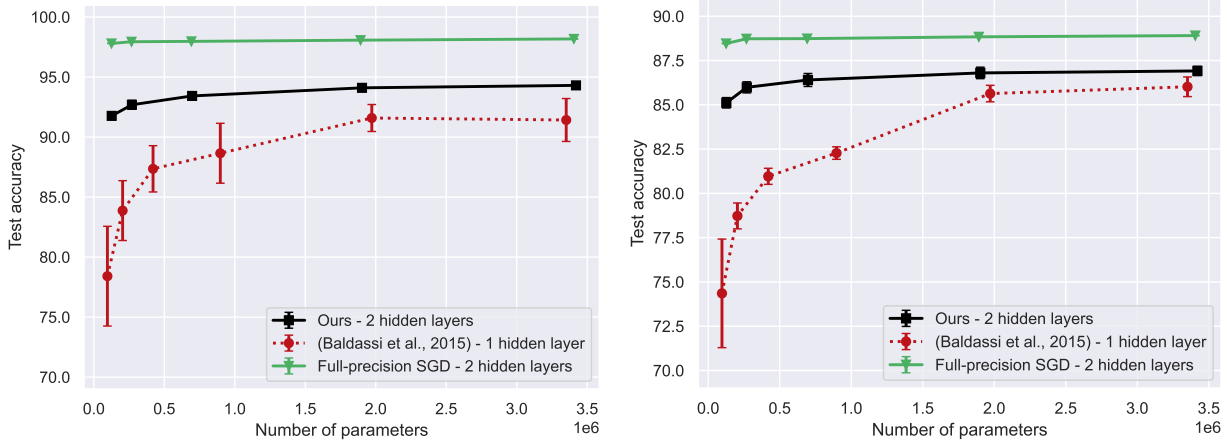
4.1.2. FashionMNIST

The second dataset is the FashionMNIST database (Xiao et al., 2017), created in 2017 as an alternative to the original MNIST dataset. FashionMNIST consists of Zalando’s articles grayscale images with a dimension of 28×28 pixels. The training dataset contains 60,000 samples, while the testing dataset includes 10,000 samples. Each image is associated with a label from 10 different classes.

4.1.3. CIFAR10

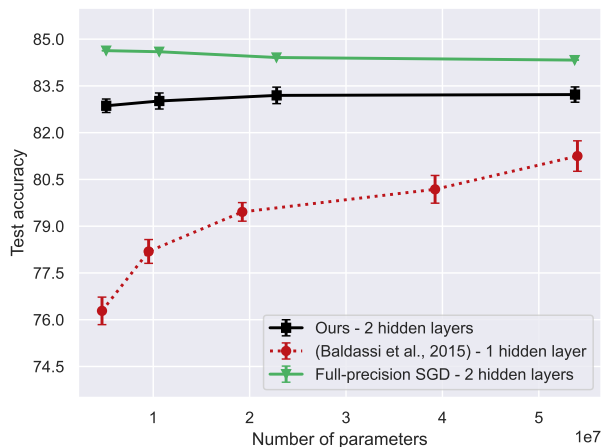
Third, the CIFAR10 (Canadian Institute for Advanced Research) dataset (Krizhevsky et al., 2009) is considered. CIFAR10 is a collection of colour images representing objects with size 32×32 belonging to 10 different classes. The dataset is divided into 50000 training samples and 10000 test samples. In particular, we considered the features extracted from a pre-trained AlexNet (Krizhevsky et al., 2017), a Convolutional Neural Network composed of five convolutional layers with ReLu activation functions (Agarap, 1803) and three max pooling layers, on which we trained a classifier through the proposed learning algorithm.

²The code will be released in the next phase.



(a) MNIST dataset

(b) FashionMNIST dataset



(c) CIFAR10 dataset

Figure 3: Test accuracy (over 10 different realizations of the initial conditions) as a function of the number of parameters, comparing a BMLP trained with our proposed solution, the single-layer solution by (Baldassi et al., 2015), and a floating-point MLP trained with full-precision SGD. The results demonstrate a significant increase in test accuracy compared to the state-of-the-art solution, particularly at smaller network sizes, with accuracy gains ranging between 6.58% and 13.36%. Additionally, only minimal degradation in test accuracy is observed when comparing our solution to full-precision SGD using the same architecture and number of parameters, ranging between 1.42% and 4.70%.

4.2. Comparison with the state-of-the-art algorithm

The objective of the first set of experiments is to compare the test accuracy of the proposed solution with the one of the state-of-the-art solution (Baldassi et al., 2015). The proposed solution is used to train two-hidden layer BNNs with the following set of hyperparameters \mathcal{H} : batch size $bs = 100$, number of epochs $e = 50$, probability of reinforcement $p_r = 0.5$, and robustness $r = 0.25$. Since the original code was not provided in (Baldassi et al., 2015), we reproduced the experiments to the best of our ability, following the description provided in the paper as accurately as possible.

Figure 3 shows the mean test accuracy over 10 different realizations of the initial conditions as a function of the number of parameters in the BMLPs. In particular, since the models have different architectures, the accuracy is provided w.r.t. the number of parameters of the BMLPs. Our proposed solution outperforms (Baldassi et al., 2015) across all the three considered datasets. The improvement in final test accuracy is particularly significant at smaller network size (i.e., around 100k parameters), resulting in gains of +13.36%, +10.76%, and +6.58% over (Baldassi et al., 2015) on the MNIST, FashionMNIST, and CIFAR10 datasets, respectively. The improvement brought by our solution w.r.t. (Baldassi et al., 2015) helps to reduce the memory footprint of the final model without compromising the final accuracy, which is a crucial aspect in resource-constrained environments. Importantly, the results obtained using our proposed solution exhibit lower variance compared to those obtained by (Baldassi et al., 2015), indicating a more stable learning procedure.

As a baseline for the comparison, we also trained two-hidden layer floating-point MLPs using full-precision SGD with the following set of hyperparameters \mathcal{H} : $bs = 100$, $e = 50$, and $\eta = 0.001$. Figure 3 shows that the loss in test accuracy of our proposed solution across the various architecture sizes is limited to -4.70% , -2.49% , and -1.42% on the MNIST, FashionMNIST, and CIFAR10 datasets, respectively. These results demonstrate that the proposed binary-native and gradient-free learning algorithm is able to train BMLPs on benchmarks with only a small degradation in final test accuracy with respect to full-precision SGD, while dramatically reducing the complexity of the operations involved in the training process.

All in all, across all tested datasets, our proposed solution not only consistently outperforms the state-of-the-art binary-native solution, but also achieves accuracies comparable to those of floating-point models trained with full-precision SGD.

4.3. The role of the group size γ

A crucial ingredient in enhancing the effectiveness of the proposed binary-native and gradient-free learning algorithm, both in the single-layer and multi-layer settings, is grouping neurons in each hidden layer into groups of size γ , as described in Section 3.3. In this second set of experiments, we demonstrate the impact of varying the group size γ on the testing results of a single-hidden layer BMLP using our proposed learning algorithm on the MNIST, FashionMNIST and CIFAR10 datasets. The hyperparameters \mathcal{H} are set as follows: batch size $bs = 100$, number of epochs $e = 50$, probability of reinforcement $p_r = 0.5$, and robustness $r = 0.25$.

Interestingly, as shown in Figure 4, which illustrates the test accuracy averaged over 10 different realizations of the initial conditions as a function of the group size γ , the optimal value γ^* is independent of the hidden layer size K_l . This implies that the optimal number of groups, hence the number of perceptrons to be updated at each step, is proportional to the hidden layer size. Therefore, there exists an optimal value of the ratio $\frac{\gamma^*}{K_l}$, or equivalently an optimal fraction of updated neurons with respect to the hidden layer size $\frac{\text{number of updated neurons}}{\text{hidden layer size}}$, which is independent of the hidden layer size itself. Furthermore, the closer γ to the optimal value γ^* , the lower the variance in test accuracy across different

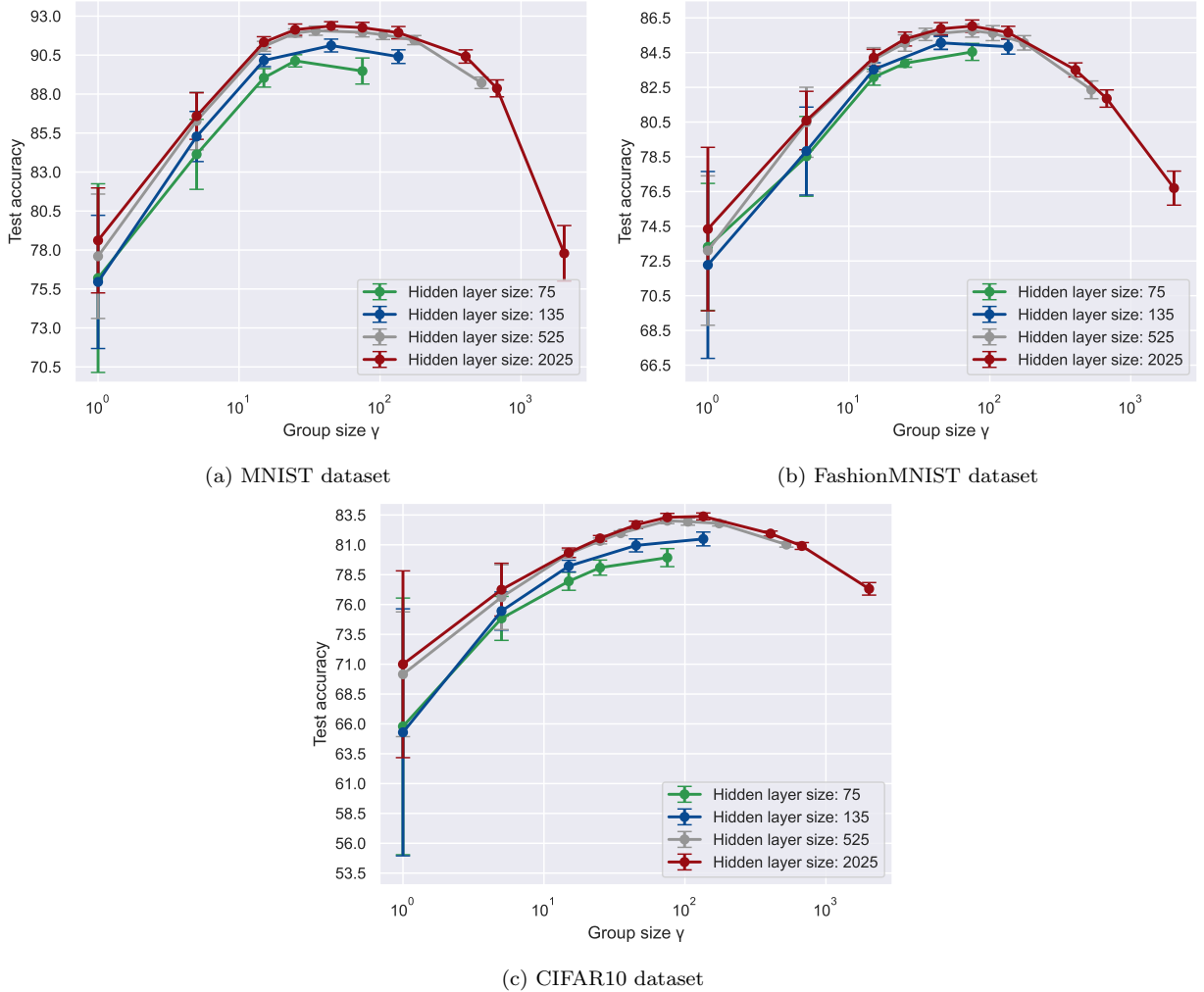


Figure 4: Test accuracy (over 10 different realizations of the initial conditions) of BMLPs trained with the proposed binary-native and gradient-free algorithm as a function of the group size γ for different hidden layer sizes. The optimal range for γ is $\Gamma^* = [65, 85]$, regardless of the hidden layer size. The closer γ to the optimal value γ^* , the lower the variance in test accuracy across different initialization, highlighting the crucial role of γ in the effectiveness and stability of the learning procedure.

initialization. This highlights the crucial role played by the group size γ not only in the effectiveness of the final BMLP but also in the stability of the learning procedure.

As shown in Figure 4, the optimal values for the group size γ range within the interval $\Gamma^* = [65, 85]$. In practice, the optimal value γ^* , for a generic layer of size K_l , is chosen as $\gamma^* = \arg \min_{\gamma \in \{\gamma | \gamma \text{ divides } K_l\}} \left| \gamma - \frac{65+85}{2} \right|$, i.e., selecting the divisor of the layer size that is closest to the optimal range Γ^* . For instance, in a model characterized by a hidden layer of size 135, γ is set to 45, resulting in the layer being divided into 3 equal-sized groups. Similarly, in a model characterized by a hidden layer of size 2025, γ is set to 75, leading to the layer being divided into 27 equal-sized groups. These values of γ implies that approximately 2.2% and 1.3% of the perceptrons in each layer are updated at every step, respectively.

It is relevant to note that, due to the permutation symmetry of the hidden layers, neurons in each group can be selected once at random before the layer-level training phase, and this selection can remain fixed throughout the learning process. We observed, however, that randomly shuffling neurons within each group at training algorithm step does not impact the effectiveness of the proposed method. In contrast, selecting a random fraction of the easiest perceptrons to update, without dividing them into sub-groups, negatively affects the performance of the algorithm. We hypothesize that grouping neurons has a regularization effect that prevents the same neurons from being updated repeatedly, thus promoting a more balanced learning process across the entire network. Further investigation of this aspect, including a rigorous analysis of the regularization effect and its impact on the learning dynamics, is left as an open problem for future research.

4.4. Ablation study: comparison with three optimized versions of the SOTA algorithm

With the aim of testing the effectiveness of our proposed solution, we conducted a broader ablation study by optimizing and modifying the SOTA algorithm (Baldassi et al., 2015) in three different ways. First, given the results obtained in Section 4.2, we modified the SOTA algorithm (Baldassi et al., 2015) by applying the group size γ optimization to the custom grouping layer employed. Second, we extended the SOTA algorithm (Baldassi et al., 2015) to deal with multi-layer BNNs by adopting LES, which allows for the efficient training of deeper architectures. Third, we combined both the optimization of the group size γ and the extension to the multi-layer scenario to create a comprehensive improvement over the original method. In particular, these three variants of (Baldassi et al., 2015) are used to train BNNs with one and two hidden layers, using the following set of hyperparameters \mathcal{H} : batch size $bs = 100$, number of epochs $e = 50$, probability of reinforcement $p_r = 0.5$, and robustness $r = 0.25$.

As demonstrated in Figure 5, which shows the test accuracy averaged over 10 different runs, the optimized versions of the algorithm from (Baldassi et al., 2015) are capable of training BNNs with both one and two hidden layers by integrating the LES procedure. Nonetheless, considering the number of parameters, our proposed solution almost always outperforms these three versions of (Baldassi et al., 2015) across all datasets. The only exception occurs on the MNIST dataset, where the group size γ optimized version of the single-layer binary algorithm of (Baldassi et al., 2015) achieves slightly higher test accuracy for BNNs with a large number of parameters. However, this behavior occurs only in this particular case and on the relatively simple MNIST dataset. For more complex tasks, and for smaller architectures, our proposed solution consistently demonstrates superior performance compared to the other analyzed algorithms.

4.5. Deep multi-layer BNNs

To demonstrate that the proposed solution is capable of training deep BNNs with more than two hidden layers, we fixed the hidden layer size K_l to 1035 and trained BNNs with a number of layers $L \in \{1, 2, 3, 5, 10\}$ by using the following set of hyperparameters \mathcal{H} : batch size $bs = 100$, number of epochs $e = 50$, reinforcement probability $p_r = 0.5$, and robustness $r_l = 0.25$. As a comparison, we trained floating-point MLPs with the same number of layers

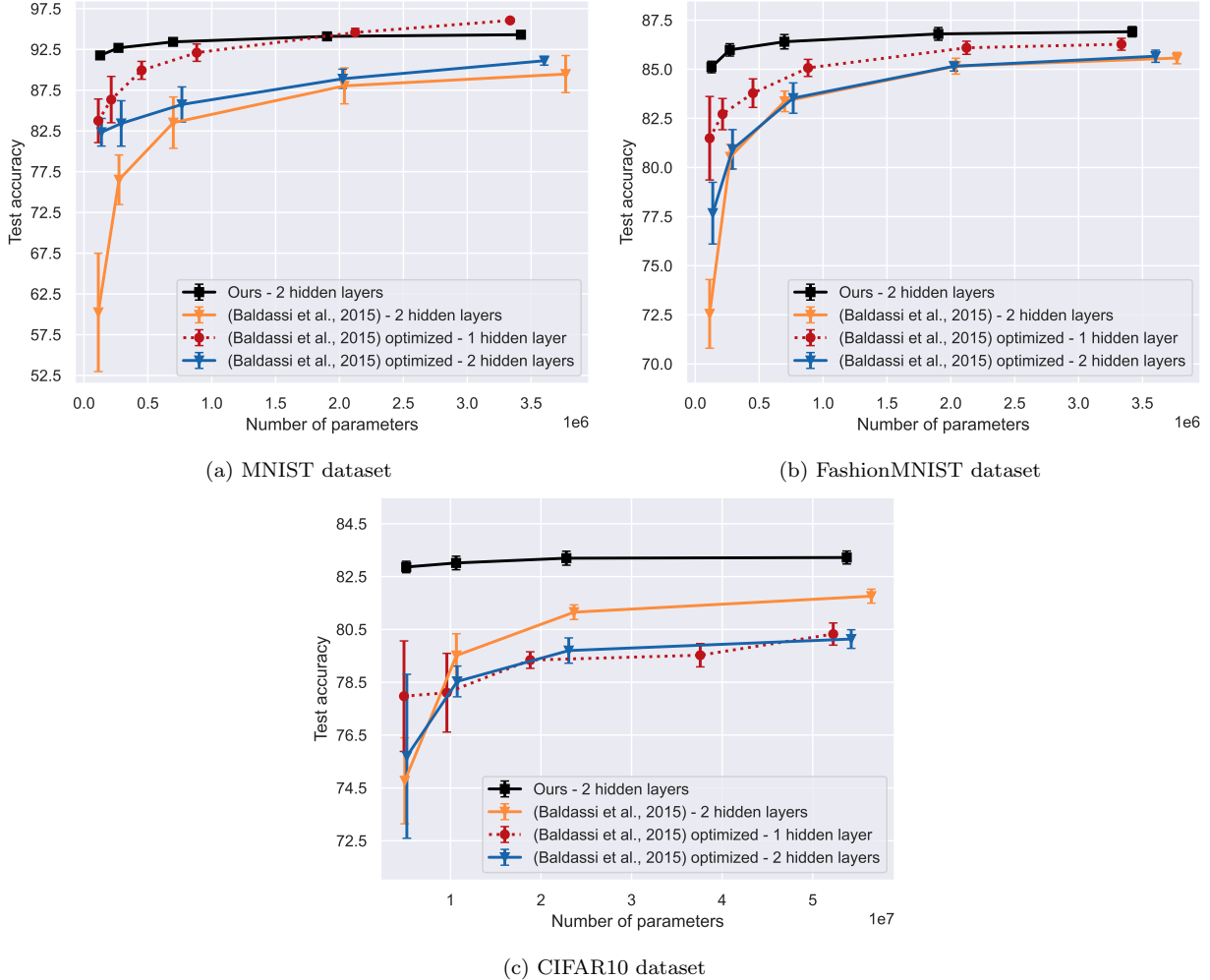
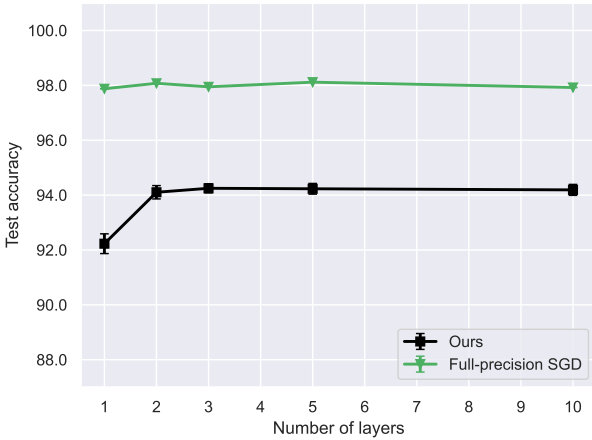


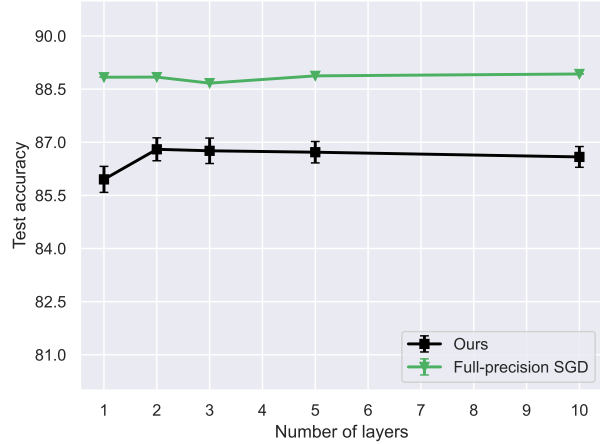
Figure 5: Test accuracy (over 10 different realizations of the initial conditions) as a function of the number of parameters for the proposed solution and the three modified and optimized versions of the algorithm from (Baldassi et al., 2015). The proposed solution consistently outperforms the other algorithms across all datasets, except for the MNIST dataset with networks having a large number of parameters. The results highlight the superior performance of the proposed method, especially on more complex tasks.

using full-precision SGD with the following set of hyperparameters \mathcal{H} : batch size $bs = 100$, number of epochs $e = 50$, and learning rate $\eta = 0.001$.

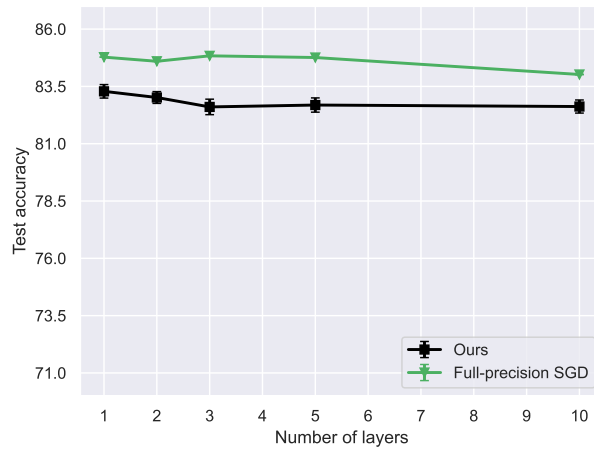
As shown in Figure 6, which illustrates the test accuracy averaged over 10 different runs, our proposed solution is able to train BMLPs with an arbitrary number of layers L . Moreover, the algorithm’s behavior of the test accuracy as a function of the number of hidden layers is comparable to that of MLPs trained with full-precision SGD, i.e., it saturates quickly with the increase in the number of hidden layers. This confirms the comparable effectiveness of our proposed solution w.r.t. SGD in managing the training of deep MLPs. We emphasize that the ability to train deep BNNs is crucial as it provides a foundational methodology for integrating other layers (e.g., convolutional layers) and extending the proposed solution to



(a) MNIST dataset



(b) FashionMNIST dataset



(c) CIFAR10 dataset

Figure 6: Test accuracy (over 10 different realizations of the initial conditions) as a function of the number of hidden layers for the proposed algorithm and full-precision SGD-trained MLPs. The proposed algorithm is capable of training BNNs with an arbitrary number of hidden layers. The algorithm’s test accuracy behavior as a function of the number of hidden layers is comparable to that of MLPs trained with full-precision SGD, confirming its effectiveness in handling the training of deep MLPs.

larger, state-of-the-art models.

5. Conclusions

In this paper we investigated the training of fully connected binary multi-layer perceptrons with binary forward and binary backward passes, by exploiting neurobiologically plausible learning rules. The proposed solution advances the current state-of-the-art by allowing the training of multi-layer BNNs without relying on the full-precision floating-point SGD-based backpropagation algorithm usually employed to train BNNs. In particular, our forward and backward steps can be computed using only XNOR, Popcount and increment/decrement operations, resulting in extreme computation and memory savings.

The application scenarios that can benefit from the binary-native and gradient-free learning of BNNs are mainly two. The first one is tiny machine learning, which targets devices with limited resources in terms of processing power, memory, and energy (Disabato and Roveri, 2020). In this case, the algorithm proposed in this paper may allow tiny devices to train ML models without relying on external Cloud infrastructures, enabling real-time processing, reducing energy consumption, and enhancing data privacy. The second scenario is privacy-preserving machine learning, which aims to protect the confidentiality of sensitive data during the training and deployment of ML and DL solutions in a *as-a-service* manner (Campbell, 2022). A promising approach in this field is represented by Homomorphic Encryption (HE), a family of cryptosystems that allows operations to be performed directly on encrypted data (Falcetta and Roveri, 2022). However, training neural networks directly on encrypted data is still impractical and requires days of computation even for small multi-layer perceptrons. To this end, being able to train and deploy DL models that only rely on Boolean arithmetic is crucial to make privacy-preserving machine learning feasible.

Future research will focus on the implementation of convolutional layers and an end-to-end backward rule akin to backpropagation in standard SGD. Additionally, a deeper analysis of the regularization effect and the impact on the learning dynamics of the group size γ will be conducted. Pure binary training, i.e., training without hidden metaplastic integer variables, will also be investigated, although we anticipate that catastrophic forgetting may be a fundamental issue in this case.

Acknowledgements

This paper is supported by PNRR-PE-AI FAIR project funded by the NextGeneration EU program.

References

- C. Thompson Neil, G. Kristjan, L. Keeheon, F. Manso Gabriel, The computational limits of deep learning, ArXiv, Cornell University, juillet (2020).
- K. Simonyan, A. Zisserman, Very deep convolutional networks for large-scale image recognition, arXiv preprint arXiv:1409.1556 (2014).
- I. Hubara, M. Courbariaux, D. Soudry, R. El-Yaniv, Y. Bengio, Quantized neural networks: Training neural networks with low precision weights and activations, journal of machine learning research 18 (2018) 1–30.
- B. Jacob, S. Kligys, B. Chen, M. Zhu, M. Tang, A. Howard, H. Adam, D. Kalenichenko, Quantization and training of neural networks for efficient integer-arithmetic-only inference, in: Proceedings of the IEEE conference on computer vision and pattern recognition, 2018, pp. 2704–2713.
- H. Qin, R. Gong, X. Liu, X. Bai, J. Song, N. Sebe, Binary neural networks: A survey, Pattern Recognition 105 (2020) 107281.

- C. Yuan, S. S. Aghaian, A comprehensive review of binary neural network, *Artificial Intelligence Review* 56 (2023) 12949–13013.
- M. Courbariaux, Y. Bengio, J.-P. David, Binaryconnect: Training deep neural networks with binary weights during propagations, *Advances in neural information processing systems* 28 (2015).
- M. Rastegari, V. Ordonez, J. Redmon, A. Farhadi, Xnor-net: Imagenet classification using binary convolutional neural networks, in: *European conference on computer vision*, Springer, 2016, pp. 525–542.
- C. Baldassi, A. Ingrosso, C. Lucibello, L. Saglietti, R. Zecchina, Subdominant dense clusters allow for simple learning and high computational performance in neural networks with discrete synapses, *Physical review letters* 115 (2015) 128101.
- C. Baldassi, Generalization learning in a perceptron with binary synapses, *Journal of Statistical Physics* 136 (2009) 902–916.
- A. Nøkland, L. H. Eidnes, Training neural networks with local error signals, in: *International conference on machine learning*, PMLR, 2019, pp. 4839–4850.
- J. Kirkpatrick, R. Pascanu, N. Rabinowitz, J. Veness, G. Desjardins, A. A. Rusu, K. Milan, J. Quan, T. Ramalho, A. Grabska-Barwinska, et al., Overcoming catastrophic forgetting in neural networks, *Proceedings of the national academy of sciences* 114 (2017) 3521–3526.
- A. Braunstein, R. Zecchina, Learning by message passing in networks of discrete synapses, *Phys. Rev. Lett.* 96 (2006) 030201. URL: <https://link.aps.org/doi/10.1103/PhysRevLett.96.030201>. doi:10.1103/PhysRevLett.96.030201.
- A. Nøkland, Direct feedback alignment provides learning in deep neural networks, *Advances in neural information processing systems* 29 (2016).
- X. Lin, C. Zhao, W. Pan, Towards accurate binary convolutional neural network, *Advances in neural information processing systems* 30 (2017).
- A. Bulat, G. Tzimiropoulos, Xnor-net++: Improved binary neural networks, *arXiv preprint arXiv:1909.13863* (2019).
- Z. Liu, W. Luo, B. Wu, X. Yang, W. Liu, K.-T. Cheng, Bi-real net: Binarizing deep network towards real-network performance, *International Journal of Computer Vision* 128 (2020) 202–219.
- Z. Tu, X. Chen, P. Ren, Y. Wang, Adabin: Improving binary neural networks with adaptive binary sets, in: *Computer Vision – ECCV 2022: 17th European Conference*, Tel Aviv, Israel, October 23–27, 2022, *Proceedings, Part XI*, Springer-Verlag, Berlin, Heidelberg, 2022, p. 379–395. URL: https://doi.org/10.1007/978-3-031-20083-0_23. doi:10.1007/978-3-031-20083-0_23.

- M. Lin, R. Ji, Z. Xu, B. Zhang, F. Chao, C.-W. Lin, L. Shao, Siman: Sign-to-magnitude network binarization, *IEEE Transactions on Pattern Analysis and Machine Intelligence* 45 (2022) 6277–6288.
- E. Vargas, C. Correa, C. Hinojosa, H. Arguello, Biper: Binary neural networks using a periodic function, *arXiv preprint arXiv:2404.01278* (2024).
- K. He, X. Zhang, S. Ren, J. Sun, Deep residual learning for image recognition, in: *Proceedings of the IEEE conference on computer vision and pattern recognition*, 2016, pp. 770–778.
- G. Huang, Z. Liu, L. Van Der Maaten, K. Q. Weinberger, Densely connected convolutional networks, in: *Proceedings of the IEEE conference on computer vision and pattern recognition*, 2017, pp. 4700–4708.
- Y. Li, S.-L. Pintea, J. C. van Gemert, Equal bits: Enforcing equally distributed binary network weights, in: *Proceedings of the AAAI conference on artificial intelligence*, volume 36, 2022, pp. 1491–1499.
- M. Rosen-Zvi, On-line learning in the ising perceptron, *Journal of Physics A: Mathematical and General* 33 (2000) 7277.
- C. Baldassi, A. Braunstein, N. Brunel, R. Zecchina, Efficient supervised learning in networks with binary synapses, *Proceedings of the National Academy of Sciences* 104 (2007) 11079–11084.
- S. Teerapittayanon, B. McDanel, H.-T. Kung, Branchynet: Fast inference via early exiting from deep neural networks, in: *2016 23rd international conference on pattern recognition (ICPR)*, IEEE, 2016, pp. 2464–2469.
- S. Scardapane, M. Scarpiniti, E. Baccarelli, A. Uncini, Why should we add early exits to neural networks?, *Cognitive Computation* 12 (2020) 954–966.
- G. Casale, M. Roveri, Scheduling inputs in early exit neural networks, *IEEE Transactions on Computers* (2023).
- C. Baldassi, Private communication, 2024.
- Y. LeCun, The mnist database of handwritten digits, *R* (1998).
- H. Xiao, K. Rasul, R. Vollgraf, Fashion-mnist: a novel image dataset for benchmarking machine learning algorithms, *arXiv preprint arXiv:1708.07747* (2017).
- A. Krizhevsky, V. Nair, G. Hinton, Cifar-10 (canadian institute for advanced research). 2009, URL <http://www.cs.toronto.edu/kriz/cifar.html> 5 (2009).
- A. Krizhevsky, I. Sutskever, G. E. Hinton, Imagenet classification with deep convolutional neural networks, *Communications of the ACM* 60 (2017) 84–90.

- A. F. Agarap, Deep learning using rectified linear units (relu). arxiv 2018, arXiv preprint arXiv:1803.08375 (1803).
- S. Disabato, M. Roveri, Incremental on-device tiny machine learning, in: Proceedings of the 2nd International workshop on challenges in artificial intelligence and machine learning for internet of things, 2020, pp. 7–13.
- M. Campbell, Privacy-preserving computation: Doomed to succeed, *Computer* 55 (2022) 95–99.
- A. Falcetta, M. Roveri, Privacy-preserving deep learning with homomorphic encryption: An introduction, *IEEE Computational Intelligence Magazine* 17 (2022) 14–25.